Electrodeposition of Ni-Fe/BN Nano-Composite Coatings from a Non-aqueous Bath and Their Characterization

Manoj Kumar Tripathi, D. K. Singh and V. B. Singh[*]

Department of Chemistry, Banaras Hindu University, Varanasi – 221 005, India
[*]E-mail: vijaybs@bhu.ac.in

Ni-Fe alloy matrix nano-composite coatings containing uniformly dispersed 24 wt% BN (boron nitride) particles (micron-sized) were electrolytically codeposited under direct current condition from a non-aqueous sulfamate-ferrous sulphate-dimethylformamide bath. Effect of various deposition parameters like Fe^{++} ion concentration, current density, temperature, stirring rate, etc. on the composition and properties of the electrodeposits was studied and optimum condition for maximum incorporation of BN particles was determined. The composite coatings thus obtained were characterized by XRD, SEM, EDAX, DSC and spectrophotometric analyses. The iron content in the alloy deposits varied between 7-25 wt%. The deposition of alloy matrix showed anomalous behaviour and was found under charge transfer and diffusion control. The calculated crystallite size of the composite deposits was found between 4-13 nm while the calculated strain in the composite coatings ranged 0.017-0.02. All the composite coatings showed fcc structure with preferred orientation in <111> crystallographic direction. The lattice parameter of the composite coatings was found to be slightly larger than that of pure nickel. Hardness of as deposited and heat treated nano-composite coatings was found to be significantly higher than that of the parent Ni-Fe alloy. A correlation between crystallite size and strain with hardness has been worked out. The hydrogen content analysis of the composites showed almost minimal hydrogen inclusion (~ 1-2 ppm) in the deposits.

1. INTRODUCTION

Nanostructured materials often exhibit outstanding properties compared with those of conventional materials and are used in a variety of applications. Though there are a number of methods like ball-milling, sol-gel, plasma spraying, PVD, CVD, lithography, etc. being employed for the preparation of composite/nano-composite materials, nevertheless electrodeposition is the method of choice for the preparation of metal matrix composites/nano-composites (MMCs), due to (i) rapidity,

(ii) low cost, (iii) easy operation, (iv) produce more compact structures, (v) high purity, (vi) wide range of controlling parameters like current density (c.d.), concentration of electrolytes, temperature, concentration of suspended particles, stirring rate, etc. (vii) no post-deposition treatment, and (viii) reproducibility. Electrodeposition is a "One step - Bottom up" approach for the preparation of nanostructures [1].

MMCs containing inert ceramic particles as reinforcement find wide range of mechanical, electronic and space applications as hard, wear resistant, thermally stable and corrosion resistant coatings [2-9]. A number of review articles on studies of MMCs have also been published [4, 10].

Hexagonal boron nitride is a soft, white, lubricious powder with graphite like structure and its layered lattice renders good lubricating property [11, 12]. It possesses electrical insulating properties, high volume resistivity (10^8-10^{13} ohm.cm), high dielectric breakdown strength (35 kV.mm^{-1}) and is resistant to heat (up to 3000 ^{o}C, dissociates) and chemicals hence corrosion resistant [13, 14]. The unique properties make it an alternative to graphite, molybdenum sulphide and other solid lubricants. The lubrication applications include additives to oil and greases, metal-ceramic electrodeposition coatings, epoxy coatings, thermal spray coatings, etc. [15]. Boron nitride being extremely stable thermally and also chemically it is environmental friendly and safe to handle.

Electrodeposited h-BN particles combined with other constituents have been used in engine parts as self-lubricating and high wear-resistance materials [16, 17]. Increased percentage of h-BN in metallic matrix composites improves hardness and wear, in spite of h-BN being soft [18, 19, 20].

Ni-Fe alloys with varying compositions from Ni-rich Permalloy to the Fe-rich Invar have variety of technological applications because of low coefficient of thermal expansion and soft magnetic properties [21, 22]. Electrodeposited nanocrystalline Ni-Fe alloys have significantly improved strength, increased wear resistance and good soft magnetic properties without compromising the coefficient of thermal expansion. These properties permit the use of Ni-Fe alloys [21] in micro-electro-mechanical systems (MEMS) since this material improves the performance of the component in terms of specific strength, elastic energy storage and thermal shock resistance, specially Ni-Fe Permalloy shows good soft magnetic properties, which are suitable to several applications such as electromagnetic shielding, read-write heads, magnetic storage devices, pole pieces of electric motors, magnetic motors, magnetic actuators, armatures in relays, and high performance transformer cores.

Electrodeposition of Ni-Fe alloy is classified as anomalous co-deposition because of the preferential deposition of the less noble metal (Fe) [23-29]. Electrodeposition of Ni-Fe alloys and their composites have been investigated by many workers [9, 30-34] using aqueous bath. It is known that the electrodeposition of metals, in aqueous media, takes place with preferential discharge of H$^+$ ions and occlusion of hydrogen which significantly affects the microstructure, crystallographic structure and mechanical properties of the metal being deposited. This hydrogen ions' discharge together with the metal deposition attracts us towards the search of suitable solvents which have no active hydrogen or in which hydrogen is more firmly bound than it is in water. Recently electrodeposition of MMCs from non-aqueous bath using N-methylformamide as solvent has been reported [2, 35] still it is a quasi-protic solvent. Electrodeposition of composites/nano-composites from organic aprotic solvents (bath) like N,N-dimethylformamide (DMF) with high donor number (26.6) and more complexing nature towards metal ions and with better wetability to the ceramic particles and lyophilic nature of BN

for DMF (better suspension) may provide deposits with better material properties in comparison to conventional aqueous bath. Therefore, it becomes obviously interesting to study the electrodeposition of metal matrix composite/nano-composite materials (Ni-Fe composites) from non-aqueous (organic) aprotic solvents.

Although substantial work has been reported on electrodeposition of Ni-Fe alloys and Ni-ceramic composites nevertheless investigations on the electrodeposition and properties of Ni-Fe alloy matrix BN composites are lacking. Therefore, it is aimed to prepare Ni-Fe/BN nano-composite coatings of desired composition (Permalloy) on Cu substrates by electrodeposition from an additive free organic non-aqueous aprotic DMF bath, their characterization and to study the effect of various controlling parameters like iron content, BN content, current density, temperature, etc. and the properties, especially mechanical, of thus prepared Ni-Fe/BN Composites.

2. EXPERIMENTAL

Ni-Fe/BN composites were prepared from an additive free bath in the laboratory by electrolytic co-deposition method. Nickel Sulfamate tetrahydrate (Fluka), Ferrous sulphate heptahydrate (Fisher Scientific, India), Boric acid (Qualigens Fine Chemicals, India), Boron Nitride powder, ~1 μm, (Sigma-Aldrich) and N,N-dimethylformamide (DMF) (Fluka) were used for preparation of electrolytic solution. All the chemicals were of analytical grade and used without further purification. The electrolysis bath composition and plating variables are given in Table-1. The electrolysis solution for Permalloy deposition was composed of 120 g/L of nickel sulfamate tetrahydrate, 1 g/L of ferrous sulphate heptahydrate, 25 g/L of boric acid while that for composite deposition contained 120 g/L nickel sulfamate tetrahydrate, 1 g/L ferrous sulphate heptahydrate, 25 g/L boric acid and varying amount (5, 10, 15, 20 g/L) of BN particles.

Table 1. Electrodeposition parameters

Parameters	Value
Nickel Sulfamate	120 g/L
Ferrous Sulphate	1 g/L
Boric Acid	25 g/L
BN powder	5-20 g/L
Solvent	DMF
Temperature	45±0.5 ^{o}C
Current Density	0.5-3.0 A/dm^2
Agitation	700 rpm

*DMF = N,N-Dimethylformamide

Commercial grade copper plates (Cu-99.28% & Ni-0.72%) of dimension 2 cm x 1 cm x 0.1 cm, used as cathode, were first mechanically polished for obtaining smooth surface, made scratch free by polishing consecutively with emery polishing papers of different grades (1/0, 2/0, 3/0 and 4/0) and finally smooth, reflective, stain free surface were obtained by disc polishing using Grade II Polishing Alumina solution (Geologists Syndicate Pvt. Ltd., India) on fine quality sylbeth cloth. Copper substrates thus obtained were washed with distilled water, methanol and then degreased in hot soap (Idipol) solution at 50^oC, washed thoroughly under running water followed by repeated washing with distilled water. The Cu strips (substrates) were dipped in acetone for a few minutes and then washed with distilled water for solvent degreasing. The strips were pickled in 10% sulphuric acid (pickling solution) then finally cleaned ultrasonically before use. The complete process and experimental setup have been described elsewhere [2, 35-37].

The highly polished copper strips were placed between two parallel rectangular plates of pure nickel anodes. A glass cell (400 mL capacity) having 200 mL of plating solution was used as the electrolysis cell. In order to obtain homogeneous suspension of BN particles in the solution (bath), the required amount of BN particles along with other electrolytes was first blended in a mortar with small amount of solvent, DMF, to get slurry and then transferred to appropriate amount of DMF and was shaken mechanically for 6 hours. The homogeneity of the suspension during electrolysis was maintained by continuous agitation with the help of two small panel fans fitted in the electrolysis cell, one on either side of the electrode, regulated by dc power supply and equipped with digital speedometer.

Before electrolysis, the solution was sonicated for 4 hours using ultrasonic cleaner (CODY, CD-2800, China). The electrolysis cell was placed in a thermostat (HAAKE DC 30, India) to maintain a uniform temperature (20-80 ^{o}C) inside the cell. The inter-electrode distance in the experiments was maintained at 2.0 cm. The electrolysis was carried out at constant current density (0.25-3.00 Adm^{-2}) for varying duration (10-90 min.) depending on the current applied. The extent of BN particles incorporation in the Ni-Fe alloy matrix was studied by varying current density and particle concentration. An optimum condition for electrodeposition was achieved by varying one parameter at a time while others kept to a fixed value.

The cathodic polarization behaviour for the deposition of metals and composite was studied by linear sweep voltametry (LSV) on CHI-660C Electrochemical Workstation (CH Instruments, USA) at a scan rate of 20 mV s^{-1} under still condition.

After the deposition, the cathode was ultrasonically cleaned for 10 minutes. XRD examination of the electrodeposited Ni-Fe/BN composites was done by Desktop X-Ray Diffractometer (Rigaku MiniFlex II) using CuKα radiation (λ = 1.541836 Å) within 20-90° 2θ Bragg's angle range. Crystallite size and strain calculations were done by the single line profile analysis of the most intense peak in the X-ray diffractogram using integral breadths as apparent crystallite size, $D = λ / β \cos θ$ [38] and strain, $η = β / 4 \tan θ$ [39], where β is integral breadth of the line and θ is corresponding Bragg's angle. Scanning electron microscope (SEM, Philips XL 20) equipped with energy dispersive X-ray analyzer (EDAX, JEOL 840A) was used to study the morphology and chemical composition of the deposits. All the chemical composition values of the deposits are quoted in weight percent (wt%), which is the average of at least five measurements. The chemical composition of the deposits was also confirmed

by spectrophotometric analysis. The wt% of Fe and Ni content was determined using sulfosalicylic acid [40] and dimethylglyoxime [41], respectively. BN content of the composite could thus be the difference between the mass of deposit and the combined mass of the metals (Ni & Fe) in the deposit. The results of spectrophotometric analysis were in good agreement with that obtained from EDAX. The hydrogen content in the deposits was measured using H_2, N_2 and O_2 analyzer (LECO TC 436). The deposited composite was vacuum sealed in a quartz glass tube and subjected to annealing at various desired temperatures between 200-700 ^{o}C. The specimen was thus heat treated for 1 hour at the desired temperature and then furnace cooled to room temperature. Differential Scanning Calorimetry (DSC) measurement of nanocomposite was performed in temperature range 30-600 ^{o}C under N_2 atmosphere with heating rate 3 ^{o}C/min on DSC822^e Mettler Toledo equipment.

Microhardness (Hv in Kgf mm^{-2}) measurement of the deposits was performed using Vickers microhardness tester (Shimadzu) at 10 g applied load for 5 s and the corresponding final values were the average of 10 measurements, avoiding any substrate effect [42].


3. RESULTS AND DISCUSSION

Influence of bath temperature and stirring rate on Ni-Fe alloy and Ni-Fe/BN nanocomposite deposition was studied qualitatively. These two parameters were optimized on the basis of adherence, smoothness and brightness of the coatings. It has been found that 45±0.5 ^{o}C bath temperature and 700 rpm stirring rate is most suitable for good quality of deposits and better suspension of the particles in the bath.

## 3.1 Effect of current density on Ni-Fe alloy and Ni-Fe/BN composite deposition

Current density is the most extensively studied parameter in electrodeposition process. Variation in current density (0.5-2.5 Adm^{-2}) affected the quality of the deposits and good quality deposits were obtained between 1.0-1.5 Adm^{-2}; at higher current densities the quality of the deposits deteriorated resulting into dull deposits with burning effect at the corners of the plates.

Fig.-1 shows the relationship between current density and Fe content in Ni-Fe alloy deposits. The Fe content in the alloy deposits decreased from 25% to 7% upon increasing current density from 0.5 Adm^{-2} to 2.5 Adm^{-2}. It can be observed from figure that iron content in the alloy decreases due to increasing the current density. However, at higher current density (>1.0 Adm^{-2}) the decrease in iron content is not sharp which indicates the impoverishment of diffusion layer in iron causing the system to come under diffusion control. It is worthwhile to note that at all current densities, the iron content in the deposits is observed to be higher than that of in the deposition bath and thus reflects the anomalous behaviour of Ni-Fe alloy deposition in DMF bath similar to aqueous bath [28].
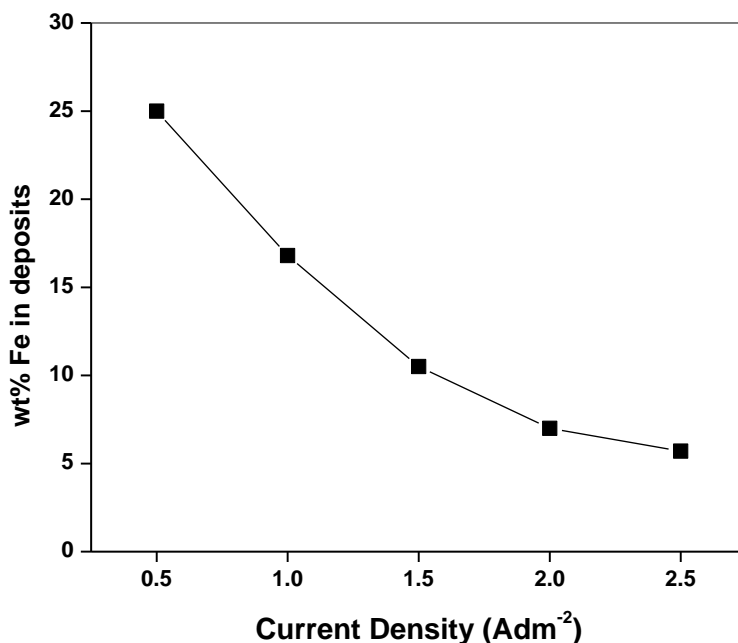
Figure 1. Variation of Fe content in the electrodeposited alloy with current density {Electrodeposition parameters : Nickel sulfamate 120 g/L, Boric acid 25 g/L, temperature 45±0.5 °C, agitation 700 rpm, without BN particles in the bath}

The current-potential curves for iron, nickel and alloy (Ni-Fe) deposition from DMF bath are shown in Fig.-2. It is observed that deposition potential for iron is nobler than nickel and for the alloy it lies in between the two.
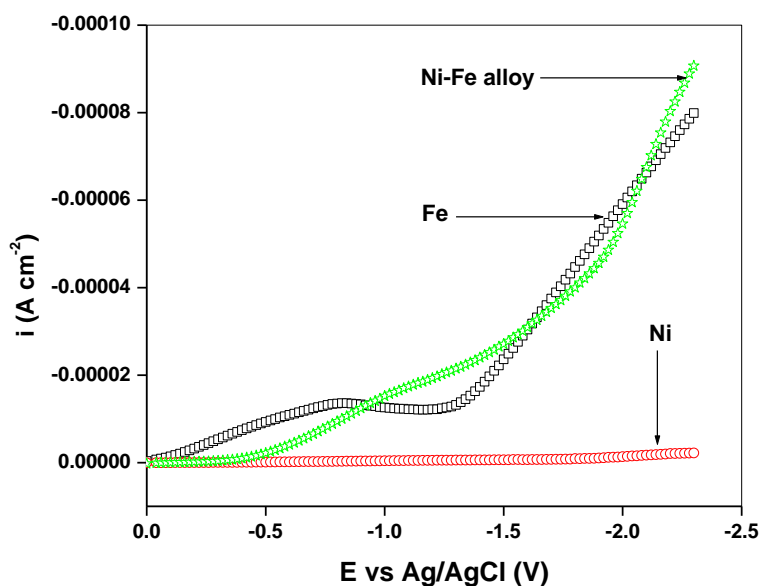
Figure 2. Polarization curves (LSV) for Fe, Ni and Ni-Fe alloy deposition in DMF bath. {Electrodeposition parameters : Nickel sulfamate 120 g/L, Ferrous sulphate 1 g/L, Boric acid 25 g/L, temperature 45±0.5 °C, without agitation}

The polarization curves clearly indicate the preferential deposition of iron over nickel and hence the deposition follows anomalous behaviour in DMF too. It is also recognized from the figure that the deposition is associated with more polarization which is due to the formation of a probable stable complexes, [43, 44, 45] i.e. $[Ni(DMF)_6]^{2+}$ and $[Fe(DMF)_6]^{2+}$ because of very high donor number of the solvent (26.6) hence high complexing nature. The complex bath usually results into fine grained deposits which have actually been observed in the present investigation.

Polarization behaviour of Fe, Ni and Ni-Fe/BN composite deposition in DMF bath containing BN particles is shown in Fig.-3. A comparison of polarization curves, (Figures-2 & 3) of metals and alloy deposition in absence and presence of suspension particles in DMF, reveals almost similar nature. These curves indicate that perhaps hydrogen is not evolved because the overpotential for hydrogen evolution (if water is considered in trace amount) is usually somewhat higher in such organic solvents than in aqueous solution. As the hydrogen ions are strongly solvated in this solvent and would discharge at a much higher potential.
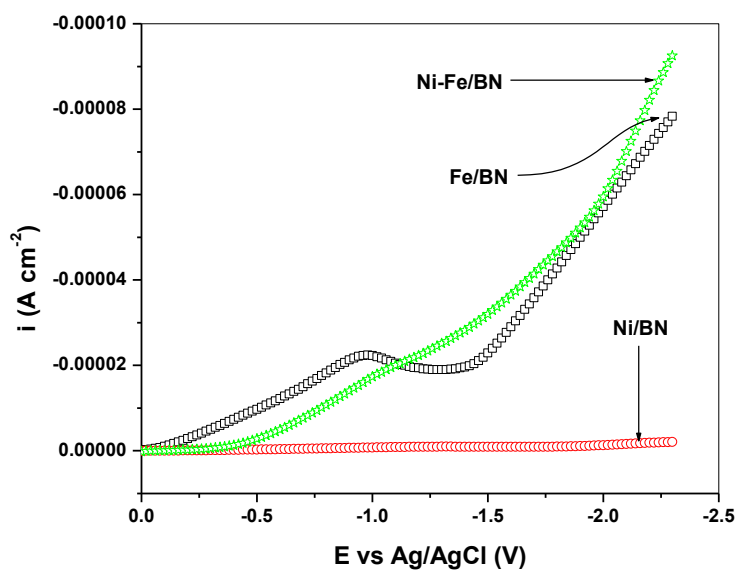
Figure 3. Polarization curves (LSV) for Fe, Ni and Ni-Fe alloy deposition in DMF bath in the presence of BN particles. {Electrodeposition parameters : Nickel sulfamate 120 g/L, Ferrous sulphate 1 g/L, Boric acid 25 g/L, BN particles 10 g/L, temperature 45±0.5 °C, without agitation}

The effect of current density on wt% incorporation of BN particles in the composite coatings is shown in Fig.-4. It is seen that the BN content in the coatings initially increased with increasing current density, reaching maximum (24 wt% BN) at 1.5 Adm^{-2}, thereafter followed a sharp decrease at 2.0 Adm^{-2}. Beyond this current density the particle incorporation tended to decrease gradually. A similar trend of variation of particle content in the composite with respect to current density has been reported earlier [10, 46].
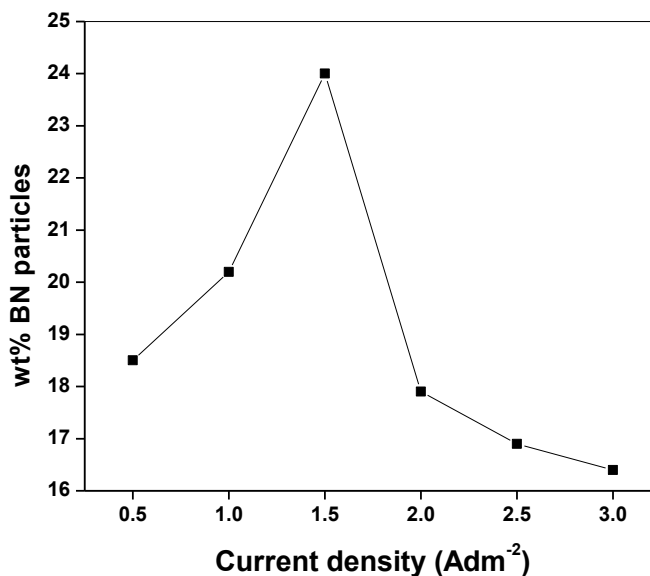
Figure 4. Variation of BN content with current density {Electrodeposition parameters : Nickel sulfamate 120 g/L, Ferrous sulphate 1 g/L, Boric acid 25 g/L, BN particles 20 g/L, temperature 45±0.5 °C, agitation 700 rpm}

The trend of variation of BN particles in the alloy composite with respect to current density is considered to be governed by the availability of particles at the cathode surface, metal ion discharge with current density and entrapment of the particles in the growing alloy. The metal ions are assumed to be adsorbed on the particle surface; hence the particle incorporation rate is directly linked with the metal deposition rate [47]. The reason for the decrease in particle content beyond a certain current density can be the switch from a kinetic to diffusion control. Once the particle was diffusion controlled, its rate remained the same as the current density increased (at 2.0 Adm^{-2}). However, the rate of metal deposition, which is still kinetically controlled, further increased with the current density, leading to a sharp decrease in particle content. The observed tendency of gradual decrease in particle content beyond 2.0 Adm^{-2} can be considered under diffusion control and metal ions discharge under mixed (kinetic as well as diffusion) control.

The trend of variation of BN particles incorporation in the composites with respect to current density can be visualized in terms of various advanced models proposed time to time [10, 48]. It emerges from the analysis of results that the present findings do not fairly conform to any single existing advanced models because of complexity of full control of the plating parameters. However, the results can be closely explained in terms of Lee and Talbot model [49].

3.2 Effect of BN particle concentration in the bath

The variation of particles concentration in bath and in deposits is shown in Fig.-5. A comparison of Figures-4 & 5 indicates that the extent of particle incorporation in the composite not only depends upon applied current density but upon the concentration of particles in the bath also. As

the BN particle concentration in the bath increases from 5 g/L to 20 g/L the incorporated particle content in the electrodeposited composite also increases from 7.2 wt% to 24.0 wt%. It seems that as the particle concentration in the bath increases more and more particles become available in the vicinity of the cathode surface leading to more incorporation in the growing metal film. However, a high particle concentration in the bath may cause their agglomeration and settling down the bottom of the bath even if being continuously agitated.
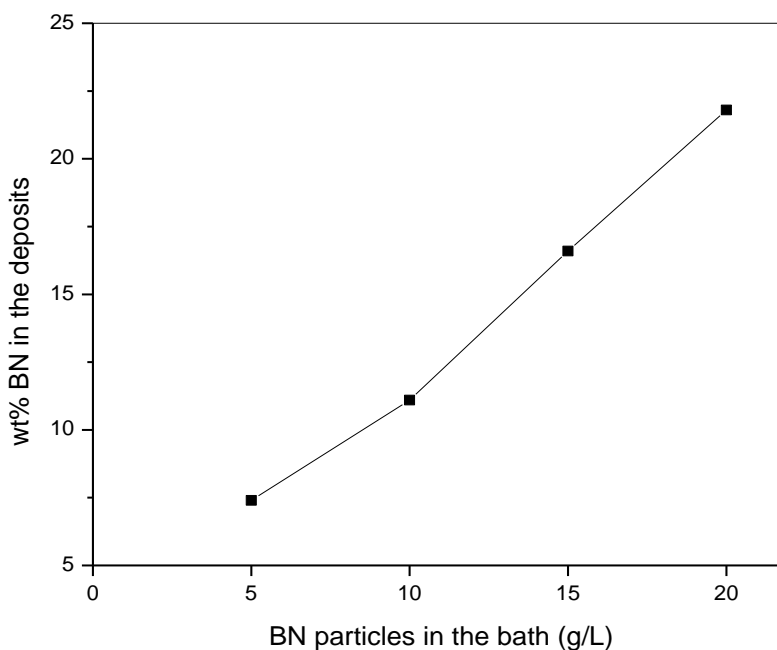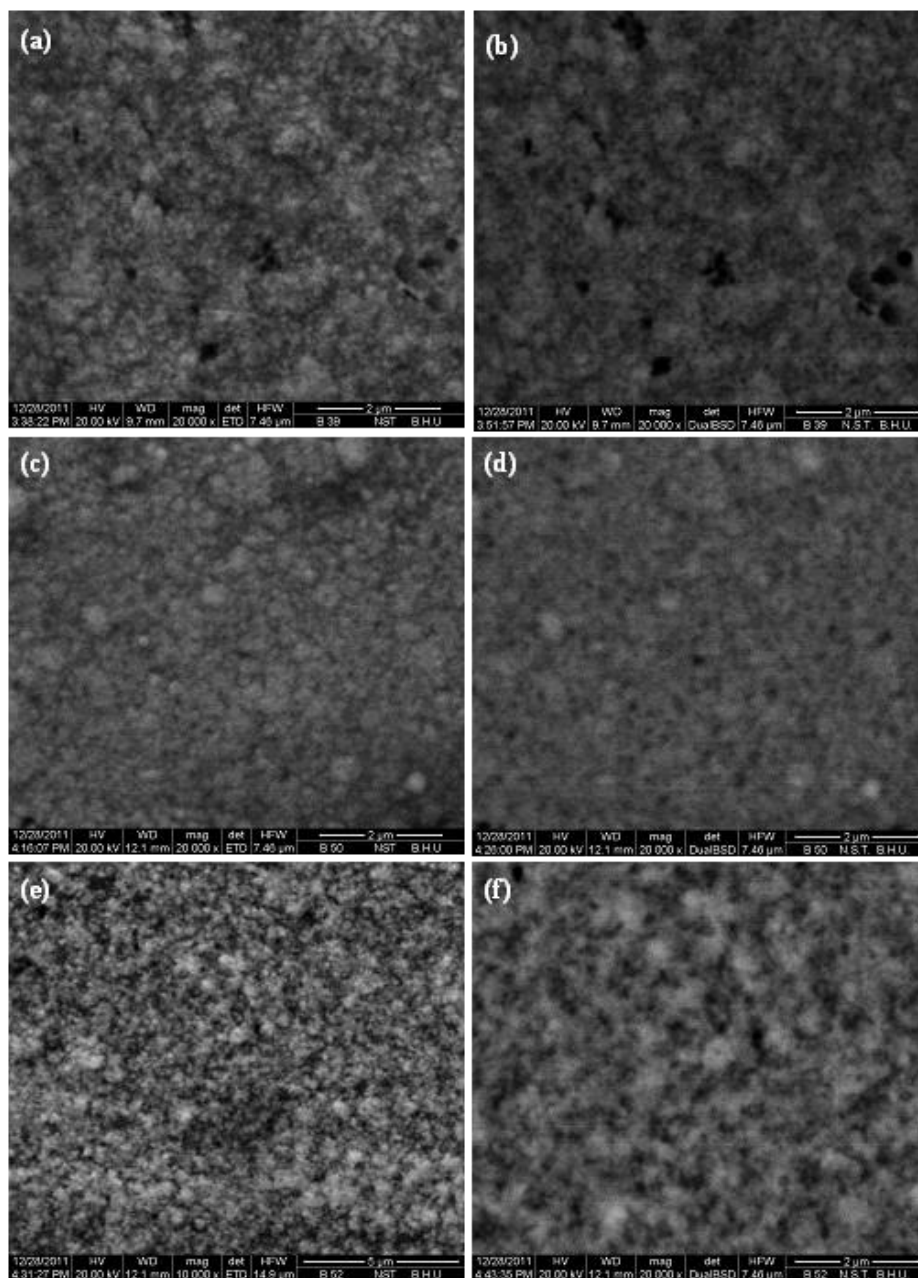

Figure 5. Variation of BN content in deposits with particle concentration in the bath {Electrodeposition parameters : Nickel sulfamate 120 g/L, Ferrous sulphate 1 g/L, Boric acid 25 g/L, current density 1.5 Adm^{-2}, temperature 45±0.5 °C, agitation 700 rpm}

3.3 SEM Study

The surface morphology of electrodeposited composite coating's was preliminarily examined by optical microscope and then under scanning electron microscope (SEM) at various magnifications. The morphological and structural characteristics of metal matrix are strongly affected by the presence of ceramic particles. Fig. 6 (a-g) represents the surface morphologies of the coatings as observed by SEM. The SEM image shows that all the deposits have very fine granular structure with uniform grain distribution. The interface between the matrix phase and the BN particles is too small to be clearly distinguished. It is apparent that the surface crystal grains of composite layer are smooth and are uniformly distributed. The measured grain size in the samples, from SEM, prepared at optimum current density, i.e., 1.5 Adm^{-2} ranged between 41-90 nm with average grain size 41.2 nm. Generally the grain diameters obtained by SEM are significantly larger than those of calculated from XRD patterns due to the fact that even small deviation from the ideal crystal will affect the coherent x-ray scattering [50]. On the other hand BN ceramic particles in the Ni-Fe alloy matrix are also uniformly

distributed throughout the matrix. The presence of BN particles in the composite coatings was also noticed in XRD results. It is evident from the SEM images that increasing concentration of BN particles in the electrolyte solution increases its incorporation in the coatings. The two phases, i.e., the matrix phase and the dispersed phase, can be distinguished easily in the SEM images (Fig. 6b, 6d, 6f, taken in backscattered mode). All the composite coatings were found to be free from pores and cracks with nearly smooth surfaces.


Figure 6. SEM images of Ni-Fe/BN composite coatings (a) c.d. 0.5 Adm^{-2}, 5 g/L BN particles in the bath, (b) backscattered image of (a), (c) c.d. 1.0 Adm^{-2}, 5 g/L BN particles in the bath, (d) backscattered image of (c), (e) c.d. 1.5 Adm^{-2}, 10 g/L BN particles in the bath, (f) backscattered image of (e). {Electrodeposition parameters : Nickel sulfamate 120 g/L, Ferrous sulphate 1 g/L, Boric acid 25 g/L, temperature 45±0.5 °C, agitation 700 rpm}
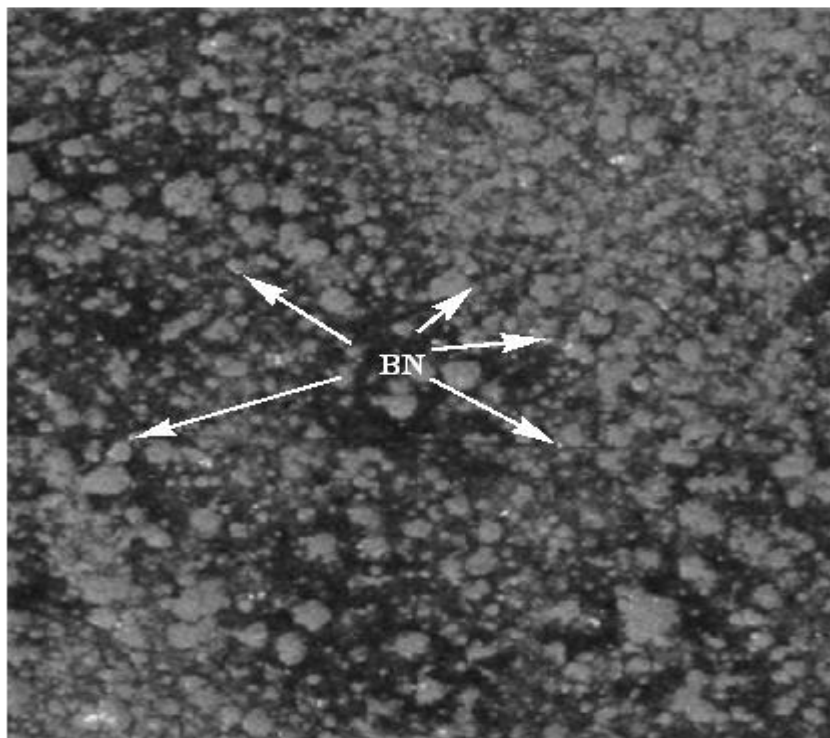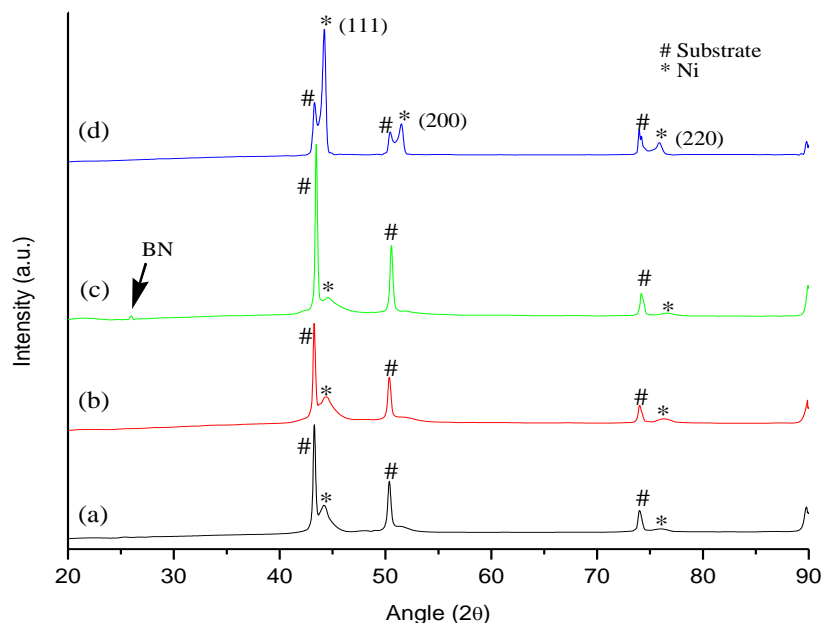
Figure 6. (g) SEM images of Ni-Fe/BN composite coatings at c.d. 0.5 Adm^{-2}, 5 g/L BN particles in the bath, {Electrodeposition parameters : Nickel sulfamate 120 g/L, Ferrous sulphate 1 g/L, Boric acid 25 g/L, temperature 45±0.5 °C, agitation 700 rpm}

3.4 XRD Study

The X-ray diffraction patterns of as deposited Ni-Fe/BN composites and vacuum annealed composites at different current densities were critically examined (Fig.-7). The XRD patterns of the composites showed crystalline fcc structures corresponding to Ni solid solution with preferred growth in <111> orientation.
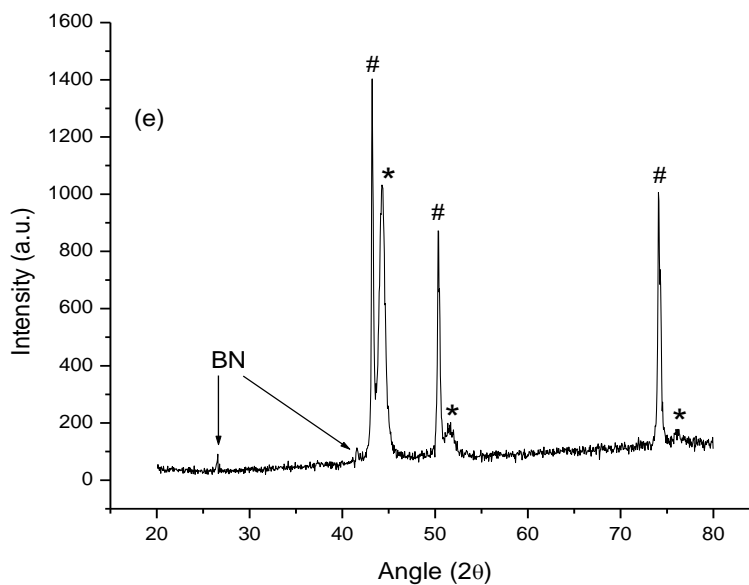
**Figure 7.** XRD pattern of as deposited Ni-Fe/BN composites (a) at 0.5 Adm[-2], (b) at 1.0 Adm[-2], (c) at 1.5 Adm[-2] and (d) annealed sample at 700 ^{o}C prepared at 1.5 Adm[-2], (e) annealed sample at 300 ^{o}C prepared at 2.0 Adm[-2] {Electrodeposition parameters : Nickel sulfamate 120 g/L, Ferrous sulphate 1 g/L, Boric acid 25 g/L, BN particles 10 g/L, temperature 45±0.5 °C, agitation 700 rpm}

All the deposits showed prominent Ni <111> and relatively low intense Ni <220> peaks. It was observed that for composites obtained at lower current densities (below 1.0 Adm[-2]) Ni <200> peak was either too weak to be observed or was missing, but it appeared in those obtained at 1.0 Adm[-2] or at higher current densities. The peaks for BN appeared at angles 26.8^o and 41.6^o 2θ with very weak intensity, to be observed in each XRD patterns, confirming the incorporation of BN particles in the alloy matrix. No characteristic peaks of other phases are identified except that for BN. It can be observed that all the electrodeposits show fcc structure with lattice parameter, 3.523 Å - 3.548 Å, which is slightly higher than that for pure nickel indicating the formation of solid solution [21].

Microstructures of the Ni-Fe alloys are dependent on the Fe content in the electrodeposits [51]. The grain size gradually decreases with increasing iron content in the deposits [52]. The crystallite size of the electrodeposited composites was calculated using the angular breadth of the Ni <111> peaks at its FWHM in conjugation with Scherrer's equation. The Gaussian function was used for curve fitting analysis for FWHM determination [53]. The diffraction peaks of the composite coatings show considerable broadening, indicating very fine grain size. It is understood that the presence of BN particles in the matrix inhibits the growth of alloy (Ni-Fe) grains and decreases the crystallite size [34].

Fig. 8 shows the variation of crystallite size with current density. It is observed that the apparent crystallite size of the deposits decreased from 13 nm to 4 nm with increasing current density from 0.5 Adm[-2] to 2.0 Adm[-2]; similar findings have been reported earlier [54, 55]. Current density plays an important role on the crystallite size of electrodeposited coatings. An increase in current density results in a higher overpotential that increases the nucleation rate thus causing grain refinement. Above a certain value of current density, depending upon the nature of the electrolyte

solution, there is no further grain refinement [56]. The calculated strain in all the coatings was observed to be minimal (~ 0.02). The calculated strains in the composite coatings are low, which can be attributed to the almost minimal hydrogen inclusion in the coatings i.e between 1-2 ppm and due to less deformation produced by the ceramic particles as the particles/crystallites are in nearly strain relaxed state.
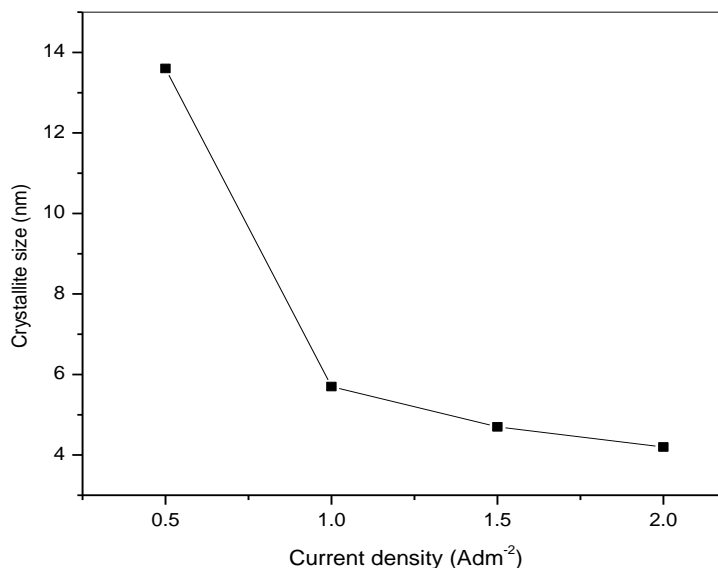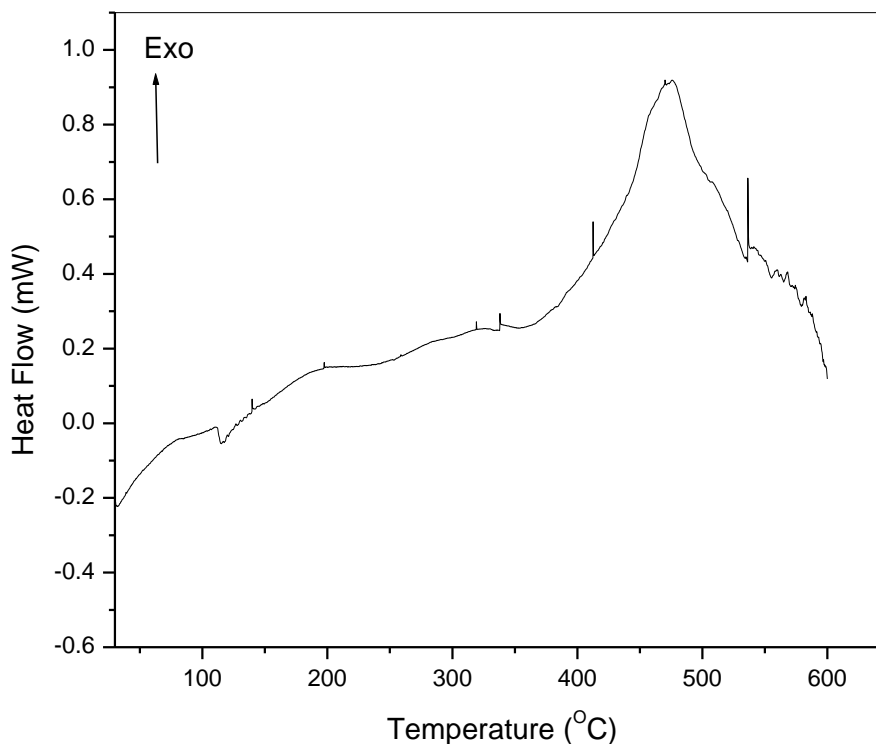

Figure 8. Variation of crystallite size with current density {Electrodeposition parameters : Nickel sulfamate 120 g/L, Ferrous sulphate 1 g/L, Boric acid 25 g/L, BN particles 10 g/L, temperature 45±0.5 °C, agitation 700 rpm}

3.5 Effect of Heat Treatment

A change in crystalline structure was observed once the composites were annealed at 700°C (1 h) (Fig. 7d). It is evident from the figure that there is preferred growth of the deposits in <111> plane on annealing, because Ni <111> plane has lowest surface energy [57], and also <200> peak significantly developed after heat treatment, which was either not visible or feeble in the as-deposited samples. This change in the peak intensities could be correlated to recrystallization and grain growth. After heat treatment up to 700 °C, an increase in lattice constant, 3.549 Å, was observed (3.524 Å in as deposited sample), which might be due to some microstructural/phase changes upon heat treatment and cooling. However, the possibility of formation of an intermetallic phase (Ni_3Fe) can not be ruled out, rather, there exists larger probability of formation of an ordered Ni_3Fe intermetallic phase in nanocrystalline Ni-Fe alloy due to the faster grain boundary diffusion [51]. Since the <111> peaks of Ni and Ni_3Fe coincide and it is difficult to resolve them, the formation of the Ni_3Fe intermetallic phase was confirmed by DSC measurements (Fig.-9), which showed a broad exothermic peak between temperature range 412-550 °C indicating disordered-ordered transition. The observed lattice constant for the intermetallic phase is close to the literature value (3.555 Å). The peak corresponding to BN remained as such after annealing whereas those of alloy shifted to a lower angles with a significant

increase in peak intensity of the <111> plane, probably representing recrystallization of the alloy [18]. The apparent crystallite size increased and found to be order of 25 nm upon annealing. This change in crystallite size is ascribed to the recrystallization and the grain growth on heat treatment. The calculated strain of the annealed samples (based on XRD data) decreased from 0.02 (before annealing) to 0.0017 (after annealing) which can be due to release in stress and lattice/grain boundary relaxation.

Figure 9. DSC trace of Ni-Fe/BN Composite {Electrodeposition parameters : Nickel sulfamate 120 g/L, Ferrous sulphate 1 g/L, Boric acid 25 g/L, BN particles 10 g/L, current density 1.5 Adm^{-2} temperature 45±0.5 °C, agitation 700 rpm}

When the deposits were annealed at low temperature, i.e. 300°C, the peak intensities corresponding to <111> and <200> planes increased while there was no appreciable change in <220> peak (Fig. 7e). Any significant change in crystallite size and lattice constant was not noticed. This is likely because low temperature annealing results in grain boundary relaxation without grain growth [58]. At the high temperature, however, the grain growth will occur toward an equilibrium state with increasing temperature. Thus the grain size dependent properties will be affected by the heat treatment.

The annealing behaviour of these materials depends strongly on the particle parameters consisting in volume fraction, size, shape and spacing of the second-phase particles. The effect of the particles on preserving the microstructure can be explained by the interaction of the particles with the grain boundaries. In fact, a dispersion of particles exerts a retarding force or pressure on a low angle or high angle grain boundary and this may have a profound effect on the process of grain growth [59].

3.6 Microhardness

The hardness values of the electrodeposited composites are given in Fig.-10. The hardness of the composite coatings ranged between 264 HV to 483 HV, and maximum value was found between current density 1.0-1.5 Adm^{-2} i.e. at maximum BN particles content. Thus, the hardness of the composite increased with increasing BN particles content in the composite, similar to the findings of others [18, 20].

The hardness of the composites increased with increasing current density up to 1.5 Adm^{-2} and thereafter declined. This might be attributed to the dispersion strengthening due to increased incorporation of BN particles in the matrix metal. The decrease in hardness after maximum follows similar trend as the particle content in the composites. Trend of variation of crystallite size (Fig.-8) and hardness (Fig.-10) with respect to current density shows dependence of hardness on the crystallite size. The hardness increases with decreasing crystallite size and attains a maximum value but below a critical size of the crystallite (5 nm) it decreases. Since strain in the materials has pronounced effect on its hardness, the hardness of nickel-rich alloy sharply increases with increasing strain up to a certain value and then decreases [60]. In the present case, all the deposited composite coatings have much less strain (~ 0.02), as calculated via XRD results. Therefore, it may be conceived that the alloying element and the ceramic phase have main contribution in the measured hardness in the coatings.
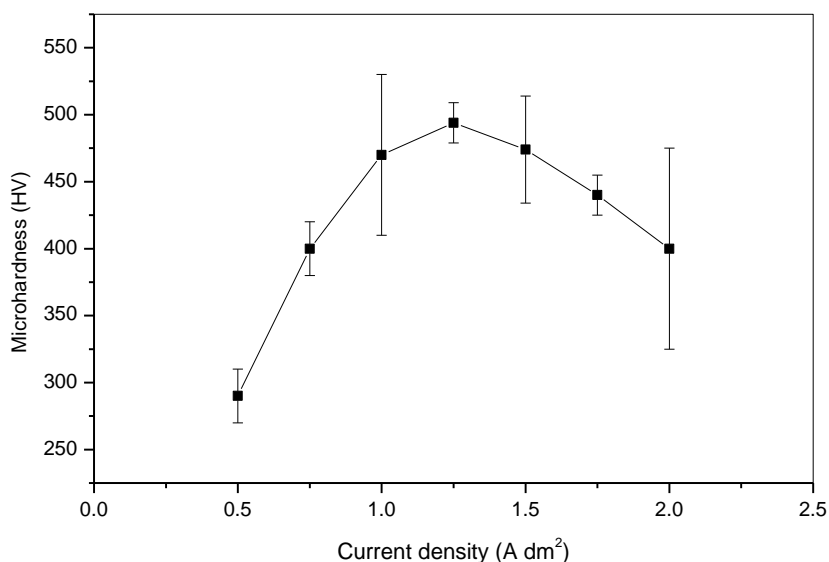
Figure 10. Variation of hardness of the electrodeposits with current density {Electrodeposition parameters : Nickel sulfamate 120 g/L, Ferrous sulphate 1 g/L, Boric acid 25 g/L, BN particles 10 g/L, temperature 45±0.5 °C, agitation 700 rpm}

The hardness of alloy composites depends upon (i) presence of alloying element (solid-solution hardening), (ii) grain size refinement (Hall-Petch hardening) and (iii) particulate reinforcement hardening (Orowan hardening or dispersion hardening). Low hardness in the deposits can be attributed

to negligible hydrogen occlusion in the composite coatings and very fine crystallite-grain size (below a certain critical limit). Smaller crystallite size implies greater number of grain boundaries that impede dislocation motion creating harder materials. Due to uniform distribution of BN particles in the composite coatings it is possible that a large number of particles situated in the grain boundaries obstruct high density of dislocations and block dislocation slippage thus increase the hardness of the coatings.

The microstructure of the electrodeposits has been identified to be nanocrystalline with an average grain size 41 nm and crystallite size below 10 nm (XRD). The remarkable increase in the hardness of Ni-Fe/BN composite coatings in comparison to pure nickel can be attributed to Hall-Petch strengthening and Orowan strengthening. Observed grain refinement of Ni-Fe matrix in the composite coating can result in a greater strengthening effect by Hall-Petch mechanism while dispersion hardening of BN particles in the Ni-Fe matrix may lead to high strengthening effect by Orowan mechanism [61].

4. CONCLUSION

Ni-Fe/BN nano-composite coatings having varying alloy composition with an average grain size of 4-13 nm containing micron sized BN particulate uniformly embedded in Ni-Fe matrix can be prepared via electrodeposition from an additive free non-aqueous (aprotic) organic bath (DMF) using nickel sulfamate-ferrous sulphate electrolytes. All the electrodeposited composites thus prepared show non-porous granular structure with <111> preferred orientation and with much less strains. The hydrogen content in the deposits can be reduced significantly to minimal level using aprotic solvent like DMF for electrodeposition. The microhardness of the composite coatings can be improved by incorporating BN ceramic particles (micron-sized) in the Ni-Fe alloy matrix.

References

1. C.C. Koch, *J. Mater. Sci*. 42 (2007) 1403.
2. V.B. Singh, D.K. Singh, *J. Electrochem. Soc*. 158(2) (2011) D114.
3. C.T.J. Low, R.G.A. Wills, F.C. Walsh, *Surf. Coat. Technol*. 201 (2006) 371.
4. A. Hovestad, L.J.J. Janssen, *J. Appl. Electrochem*. 25 (1995) 519.
5. L. Benea, P.L. Bonora, A. Borello, S. Martelli, *Wear* 249 (2002) 995.
6. I. Garcia, J. Fransaer, J.P. Celis, *Surf. Coat. Technol*. 148 (2001) 171.
7. P. Gyftou, M. Stroumbouli, E.A. Pavlatou, P. Asimidis, N. Spyrellis, *Electrochim. Acta.* 50 (2005) 4544.
8. G. Sharma, R.K. Yadava, V.K. Sharma, *Bull. Mater. Sci*. 29(5) (2006) 491.

9. H. Ataee-Esfahani, M.R. Vaezi, L. Nikzad, B. Yazdani, S.K. Safrnezhaad, *J. Alloys. Compd*. 484 (2009) 540.
10. J.L. Stojak, J. Fransaer, J.B. Talbot, Review of Electrodeposition in : R.C. Alkire and D.M. Kolb (Eds), Advances in Electrochemical Science and Engineering, Vol. 7, Wiley-VCH Verlag GmbH (2001), pp 193-223 ISBN: 3-527-29830-4.
11. D.A. Lelonis, (1994) Boron Nitride-A Review, Ceramic Technology International, A Sterling Publication; Ceramic Industry Materials Handbook, January 1998 : 79.
12. L. Ploof, *Adv. Materials & Processes*, May (2008) 36.
13. H. Sliney, Solid Lubricants, NASA Technical Memorandum (1991) 102803.
14. B. Erhan, B. Cetin, *J. Solid. State. Chem*. 177(4/5) (2004) 1768.
15. S. Zhang, J. Zhou, B. Guo, H. Zhuo, Y. Pu, J. Chen, *Mater. Sci. Eng.* A 491(1/2) (2008) 47.
16. T. Urushibara, Japan Patent (1992) 04263095.
17. Y. Harakawa, Japan Patent (1982) 57089499A.
18. M. Pushpavanam, S.R. Natarajan, *Metal Finishing* June (1995) 97.
19. G. Bapu, *Plating and Surface Finishing*, July (1995) 70.
20. E. Pompei, L. Magagnin, N. Lecis, P.L. Cavallotti, *Electrochim. Acta* 54 (2009) 2571.
21. J.L. McCrea, G. Palumbo, G.D. Hibbard, U. Erb, *Rev. Adv. Mater. Sci.* 5 (2003) 252.
22. R. Abdel-Karim, Y. Reda, M. Muhammed, S. El-Raghy, M. Shoeib, H. Ahmed, *J. Nanometerials* (2011) (DOI : 10.1155/2011/519274).
23. K. Nakamura, M. Umetani, T. Hayashi, *Surf. Technol*. 25 (1985) 111.
24. K.H. Wong, P.C. Andricacos, L.T. Romankiw, Proc. Second Int. Symp. Mag. Materials, Processes, Devices, Eds. L.T. Romankiw & D.A. Herman Jr. The Electrochem. Soc. NJ (1990) 387.
25. D. Gangasingh, J.B. Talbot, *J. Electrochem. Soc*. 138 (1991) 3605.
26. S.S. Djokic, M.D. Maksimovic, Electrodeposition of Ni-Fe alloys in: J. O'M. Bockris (Ed.), Modern Aspects of Electrochemistry, Plenum Press, New York (1992), No. 22, pp. 417.
27. K.M. Yin, B.T. Lin, *Surf. Coat. Technol*. 78 (1996) 205.
28. A. Brenner, Electrodeposition of alloys : Principles and practice, Vol. II, Academic Press, New York and London (1963).
29. A. Afshar, A.G. Dolati, M. Ghorbani, *Mater. Chem. Phys*. 77 (2002) 352.
30. D. Singh, V.B. Singh, *Ind. J. Technol*. 13 (1975) 520.
31. C. Cheung, G. Palumbo, U. Erb, *Scr. Metall. Mater*. 31(6) (1994) 735.
32. S. Gadad, T. Harris, *J. Electrochem. Soc*. 145(11) (1998) 3699.
33. X. Li, Li Zhiwei, *Mater. Sci. Eng.* A 358 (2003) 107.
34. Y. Marita, I.I. Yaacob, Proc. World Cong. Eng. Vol. II July 2-4, London UK (2008), ISBN:978-988-17012-3-7.
35. V.B. Singh, D.K. Singh, *Mater. Sci. Eng*. A 532 (2012) 493.
36. V.B. Singh, R.S. Sarabi, *Plat. Surf. Finish*. 83 (1996) 54.
37. V.B. Singh, P. Pandey, *Surf. Coat. Technol*. 200 (2006) 4511.
38. P. Scherrer, *Gott. Nachr*. 2 (1918) 98.
39. T.H.D. Keijser, J.I. Langford, E.J. Mittemeijer, A.B.P. Vogels, *J. Appl. Cryst*. 15 (1982) 308.
40. Vogel's Textbook of Quantitative Chemical Analysis 6th Edn., Eds. J. Mendham, R.C. Denney, J.D. Barnes, M. Thomas; Pearson Education Asia (2003), pp. 394.
41. A.I. Vogel, A Textbook of Quantitative Inorganic Analysis. Longmans, Green & Co, London (1956) pp 794
42. H.E. Boyer, (Ed) Hardness Testing, ASM International, Metals Park, OH (1987).
43. T. Takei, *Bull. Chem. Soc. Jpn*. 47 (1974) 257.
44. T.A. Silinskaya, S.V. Volkov, N.I. Buryak, *Ukr. Khim. Zh.* 68(3) (2002) 35.
45. O.I. Kuntyi, E.V. Okhremchuk, M.S. Khoma, *Materials Science* 39(6) (2003) 885.
46. J.L. Stojak, J.B. Talbot, *J. Electrochem. Soc*. 146 (1999) 4504.

47. J.P. Celis, J.R. Roos, C. Buelens, *J. Electrochem. Soc.* 134(1987) 1402.
48. A. Hovestad, L.J.J. Janssen, Electroplating of Metal Matrix Composites by Codeposition of Suspended Particles. In : B.E. Conway et al. (Eds.) Modern Aspects of Electrochemistry, 38th edn. Kluwer Academic/Plenum Publishers, New York, 2005, pp 475-532.
49. J. Lee, J.B. Talbot, *J. Electrochem. Soc.* 154 (2007) D70.
50. P. Angerer, H. Simulkova, E. Schafler, M.B. Kerber, J. Wosik, G.E. Nauer, *Surf. Coat. Technol*. 203 (2009) 1438.
51. H. Li, F. Ebrahimi, *Mater. Sci. Eng*. A 347 (2003) 93.
52. D.L. Grimmett, M. Schwartz, K. Nobe, *J. Electrochem. Soc*. 140 (1993) 973.
53. A. Sanaty-zadeh, K. Raeissi, A. Saidi, *J. Alloy Compd*. 485 (2009) 402-407.
54. J. W. Dini, Electrodeposition : The Material Science of Coatings and Substrates, Noyes Publications New York (1993).
55. R. Winand, *Electrochim. Acta* 39 (1994) 1091.
56. L. Wang, Y. Gao, T. Xu, Q. Xue, *Mater. Chem. Phys*. 99 (2006) 96.
57. H. Li, F. Czerwinski, J.A. Szpunar, *Nanostr. Mater*. 9 (1997) 673.
58. M. Thuvandr, M. Abraham, A. Cerezo, G.D.W. Smith, *Mater. Sci. Technol*. 17 (2001) 961.
59. F. Humphreys, M. Matherly, Recrystallization and Related Annealing Phenomena, Oxford, UK: Elsevier, 2004, ISBN 0-08-044164-5.
60. H.T. Ni, X.Y. Zhang, P.Y. Li, *Mater. Sci. Eng*. A 538 (2012) 302.
61. W. Wang, F. Hou, H. Wang, H. Guo, *Scripta Materialia* 53 (2005) 613.